Monolayer Films of Poly(dimethylsiloxane) on Aqueous Surfactant Solutions

V. Bergeron*

Laboratorie de Physique Statistique, Ecole Normale Supérieure, 24, rue Lhomond, 75231 Paris Cedex 05, France

D. Langevin

Centre Recherche Paul Pascal, Avenue A. Schweitzer, 33600 Pessac, France

Received March 13, 1995; Revised Manuscript Received September 28, 1995[⊗]

ABSTRACT: Spreading at the air−solution interface, of poly(dimethylsiloxane) (PDMS), a widely used ingredient in commercial antifoaming agents, depends strongly on the type of surfactant dissolved in solution. To isolate which polymer−surfactant interactions control the process, we measure surface pressure isotherms for PDMS on a wide variety of surfactant solutions. Moreover, we directly probe the influence of electrostatic forces by addition of a 1:1 electrolyte to the solutions. Although surfactant type, anionic, cationic, or nonionic, and level of charge play only a minor role, the length of the surfactant tail can control the PDMS spreading behavior. For the homologous series of alkyltrimethylammonium bromides, a critical carbon chain length of 14 is found, above which PDMS displays "complete" wetting behavior. However, shorter chain lengths can induce a metastable condition of "pseudopartial" wetting. We utilize both two dimensional polymer scaling concepts and generalized spreading coefficients to rationalize our results.

Introduction

Antifoaming and defoaming agents are important to a wide range of industrial applications.[1] Although the theoretical understanding of these agents has progressed substantially in the past 2 decades, there are still major gaps in our understanding of precisely how they work. Often is the case that an agent will work well for one system but fail for another. Moreover, it is well-known that the effectiveness of an antifoaming agent can diminish with time.[2] Therefore, in order to understand and utilize these agents more efficiently, we need fundamental, systematic studies to identify the key mechanisms that take place during defoaming operations.

The most common ingredient used in commercial antifoaming and defoaming agents is poly(dimethylsiloxane) (PDMS). Typically, this insoluble polymeric oil is combined with microscopic (<1 μm) silica particles to form a solid−oil hydrophobic mixture that emulsifies into small droplets (>10 μm) when added to aqueous surfactant solutions. These small droplets then bridge the individual foam lamella, which subsequently leads to film rupture and hence foam destruction. Essentially two mechanisms are believed responsible for the film's rupture; oil spreads at the air−water interface producing film thinning via subsurface fluid entrainment, and flow out of the film is driven by finite contact angles created at the border between the hydrophobic surface of the antifoaming droplet and the foam lamella.[3] Both of these mechanisms seem to be firmly established; however, the conditions needed to promote them still requires a deeper understanding of the processes involved. To achieve this, we must first identify the fundamental aspects of the process and then systematically investigate each component. In particular, for the important commercial agents, a thorough understanding of the polymer (PDMS)−surfactant interactions in foaming systems is required. Hence, this paper focuses on the PDMS−surfactant interactions at the air−solution interface.

Our work is motivated by the preliminary studies of Mann et al.[4,5] In their work the submonolayer spreading behavior of PDMS on two different surfactant solutions is studied, namely, aerosol-OT (AOT), a double-chain anionic surfactant and penta(ethylene glycol) mono-*n*-decyl ether ($C_{10}E_5$), a single-chain nonionic surfactant. They find that the PDMS spreading behavior on these two solutions is very different; however, the structure of the surfactants used is too diverse to definitively conclude which surfactant properties create the observed differences. Nevertheless, the work of Mann et al. does serve as an excellent starting point for a more systematic study. To accomplish this, we use the homologous series of alkyltrimethylammonium bromide surfactants, $C_nH_{2n+1}N(CH_3)_2Br$ (i.e., C_nTAB), where n = 9, 10, 12, 14, 16. With this cationic surfactant series, in combination with AOT and $C_{10}E_5$ solutions, we investigate both surfactant chain length and headgroup charge effects on the spreading behavior of PDMS monolayers. Moreover, ionic interactions are directly probed by regulating the electrostatic screening length via the addition of a 1:1 electrolyte to the solutions.

The work by Mann et al. includes a variety of different methods to probe the PDMS monolayer behavior at the air−solution interface. Utilizing Brewster angle microscope (BAM) images and neutron reflectivity measurements, they establish two different types of PDMS submonolayer behavior; either the polymer separates into inhomogeneous dilute and dense phases (e.g., AOT−solution interface) or it forms a uniform homogeneous layer (e.g., $C_{10}E_5$−solution interface). In addition, Mann et al. correlate their BAM and spectroscopic observations with changes in the surface tension versus PDMS surface concentration isotherms. These isotherms are tantamount to measuring the surface pressure isotherms for single component systems. Their correlations reveal that the slope of the surface tension isotherms can be used to characterize the different PDMS submonolayer spreading behavior observed in

[⊗] Abstract published in *Advance ACS Abstracts,* December 1, 1995.

0024-9297/96/2229-0306$12.00/0

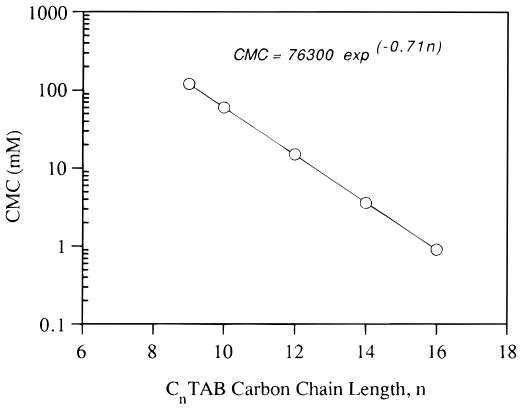

Figure 1. Critical micelle concentration (cmc) versus carbon chain length, *n*, for alkyltrimethylammonium bromide surfactants at 21 °C and in the absence of added electrolyte.

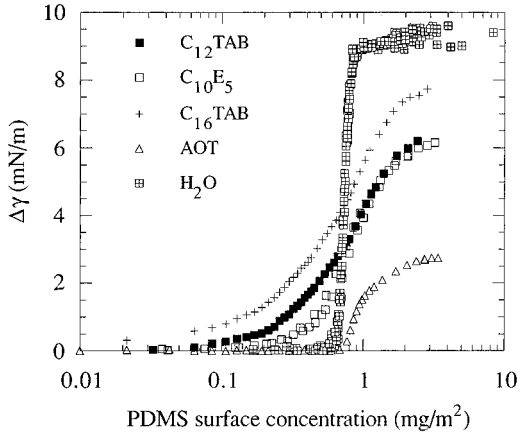

Figure 2. Change in surface tension as a function of PDMS surface concentration for various surfactant solutions. All surfactant solutions are set at 3 times the air−solution cmc, at 21 °C.

the BAM images. Large slopes in the isotherm correspond to surfaces in which PDMS does not easily spread; instead it produces islands of densely packed PDMS separated by regions of dilute PDMS or a fresh air−solution interface. Conversely, a small slope in the isotherm indicates a surface in which PDMS is homogeneously distributed on the surface. The difference in the spreading behavior is controlled by the polymer−substrate interactions, which in the present case change when PDMS is spread on different surfactant solutions. These observations can be rationalized by two dimensional polymer scaling concepts which predict a decreasing slope in the surface pressure isotherm when the polymer spreads more easily on the surface (4−13). Therefore, we utilize these concepts and measure the change in the surface tension ($\Delta\gamma = \sigma$(pure water) − σ(PDMS covered)) versus PDMS surface concentration, on different surfactant solutions, to systematically investigate which surfactant properties are most important for the equilibrium spreading of PDMS at the air−solution interface.

Experimental Section

Materials. The PDMS oil used in this study, 47v 100, M_w = 10 000 (M_w/M_n = 1.8) was supplied by Rhône Poulenc and has been treated to remove low molecular weight oligomers. The anionic surfactant, AOT, was purchased from Sigma, and the cationic alkyltrimethylammonium bromide surfactants were obtained from Kodak. C_{12}TAB was twice recrystallized with a 10:1 ethyl acetate:ethanol mixture, while the other alkyltrimethylammonium bromides were recrystallized two or three times in 50:50 wt % acetone:methanol solutions. The nonionic surfactant, penta(ethylene glycol) mono-*n*-decyl ether ($C_{10}E_5$), was used as received from Nikkol. Surface tension versus surfactant concentration isotherms for all of the surfactants used showed no sign of a minimum, indicating a high level of purity. Furthermore, as seen in Figure 1, the critical micelle concentration (cmc) values obtained for the alkyltrimethylammonium bromide series obey the expected logarithmic relationship with increasing chain length and show excellent agreement with literature values.[14,15] Sodium chloride (NaCl) and potassium bromide (KBr, *Gold Label*) were purchased from Aldrich and heated to 500 °C for several hours to drive off surface active impurities. Finally, all solutions are prepared with water taken from a Millipore-MilliQ ultrapure water system.

Surface Tension Isotherms. All experiments were performed at ambient temperature, 21 ± 1 °C. Surface tension experiments at the air−solution interface where performed via the Wilhelmy method using a rectangular (20 mm × 10 mm), "open-frame" probe made from platinum wire (0.19 mm in diameter) attached to a sensitive, Hottinger Baldwin Messtechnik (HBM) Type Q11 force transducer. The open-frame probe eliminates anomalies seen when using other probe geometries on insoluble polymer layers (e.g., plate, ring) and reproducibility with this system is better than ±0.06 mN/m. The air−solution surface tension measurements are conducted in a Teflon trough (350 mm × 70 mm × 5 mm) that is enclosed in a Plexiglas box to prevent contamination and to maintain a humidified environment. The Teflon trough, platinum probe, and all glassware are cleaned with sulfochromic acid and rinsed with copious amounts of Millipore-MilliQ purified water.

For equilibrium, surface tension, $\Delta\gamma$, versus PDMS surface coverage experiments, the method "successive additions" is applied. That is, the polymeric oil is first dissolved in ultrapure hexane (0.1 mg of PDMS/(mL of hexane)) and then applied to the surface with a microliter syringe in 5 μL aliquots. In some cases, chloroform instead of hexane is also used as a spreading solvent to ensure that the results are not affected by the nature of the spreading solvent. After the PDMS−solvent solution is applied, sufficient time (>5 min) is given for the spreading solvent to evaporate and to establish equilibrium conditions before a surface tension measurement is made.

Interfacial Tensions. Values for the interfacial tension between PDMS oil and the aqueous solutions are required to determine the classical spreading coefficients for each oil−solution combination. However, due to probe wetting difficulties, the Wilhelmy method proved unreliable for this purpose and instead we use the drop-weight method to measure the interfacial tensions. Both oil drops grown in water and water drops in oil where utilized. With correction factors from Harkins and Brown[16] and Wilkinson,[17,18] this method worked well for our systems and we were able to measure interfacial tensions to an accuracy of ±0.5 mN/m.

Results

Surfactant Type. Figure 2 displays the results obtained for $\Delta\gamma$ (mN/m) versus the concentration of PDMS (mg/m^2) on the surface of water and for a variety of surfactant solutions. All surfactant concentrations were set at three times the cmc to provide a surfactant-saturated, air−solution interface. A portion of the data shown for $C_{10}E_5$ and for water was taken directly from Mann et al.,[4,5] and we note that our new data reproduce that data very well. The data set for each solution is assigned its own symbol, and the key can be found directly on the graph. Qualitatively the curves appear similar; they all have the characteristic "s" shape displayed by many insoluble monolayers. This form has also been observed by Banks, for PDMS spreading on organic liquid substrates.[19] Moreover, the rise in all the curves is centered near a PDMS surface concentration of 0.75 mg/m^2. However, two distinct differences can

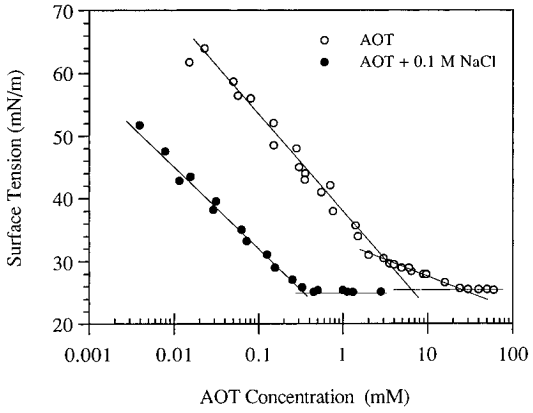

Figure 3. Surface tension versus concentration of AOT, with and without 0.1 M NaCl, at 21 °C.

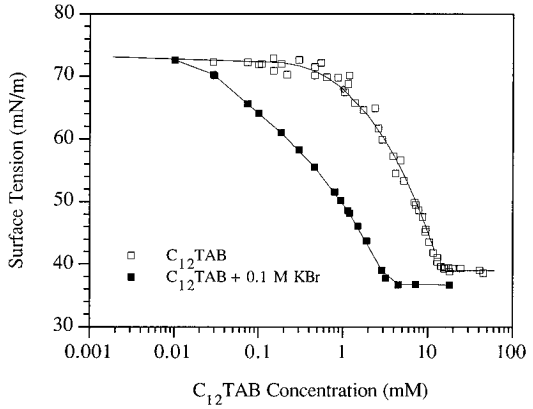

Figure 4. Surface tension versus concentration of $C_{12}TAB$, with and without 0.1 M KBr, at 21 °C.

be noted: the slope and the final plateau value for $\Delta\gamma$ change with changing surfactant solution.

Addition of Salt. To investigate the effect ionic head-group interactions have on the spreading PDMS monolayer, we add 0.1 M KBr to the cationic surfactant, $C_{12}TAB$, and 0.1 M NaCl to the anionic surfactant, AOT. Addition of electrolyte substantially influences these systems, as can be seen by comparing the open symbols (no salt) and filled symbols (0.1 M salt) of the surface tension isotherms in Figures 3 and 4. The effect is witnessed by the change in slope of the isotherms and the lowering of both the surface tension and surfactant concentration value at the cmc. The lines shown in Figures 3 and 4 correspond to polynomial fits. The electrolyte in these solutions effectively neutralizes the charged heads and screens the electrostatic contributions to the molecular interactions. This results in a slightly higher surfactant density at the surface and will also diminish any electrostatic forces between the spreading polymer and the surfactant head groups. Application of the Gibbs adsorption equation[20] to the surface tension data allows us to determine the surfactant molecular surface area at the cmc. For $C_{12}TAB$ we find 44 Å^2/molecule, and when 0.1 M KBr is present, this value is reduced to 33 Å^2/molecule. AOT areas are considerably larger at 115 Å^2/molecule without salt, with a reduction to 75 Å^2/molecule upon adding 0.1 M NaCl.

PDMS "surface pressure" results on AOT solutions are presented in Figure 5, while Figure 6 contains the data on $C_{12}TAB$ solutions. In both figures, the open circles correspond to data for solutions that only contain surfactant and the filled squares represent data for solutions with 0.1 M added electrolyte. Again, we note

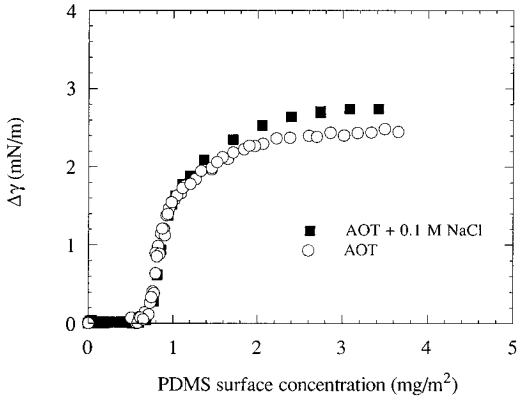

Figure 5. Change in the surface tension versus PDMS surface concentration on AOT solutions (at surfactant concentrations of 3 times the cmc), with and without 0.1 M NaCl, at 21 °C.

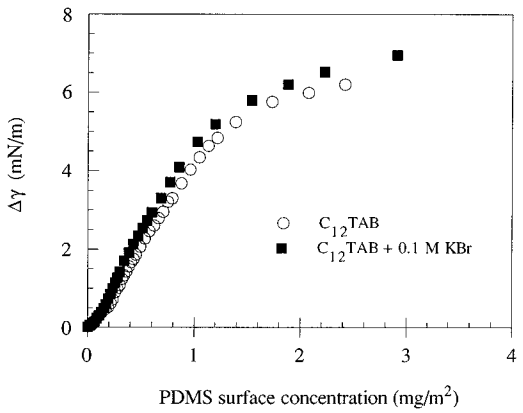

Figure 6. Change in the surface tension versus PDMS surface concentration on $C_{12}TAB$ solutions (at surfactant concentrations of 3 times the cmc), with and without 0.1 M KBr, at 21 °C.

that, for the PDMS spreading isotherms using these surfactants, the surfactant concentration is fixed at three times the cmc, which is adjusted correspondingly for the addition of salt. As can be seen in the figures, the addition of salt has very little effect on the isotherms. There is a slight elevation of the $\Delta\gamma$ plateau value in both cases, but no appreciable differences are observed below 1.2 mg/m^2 of PDMS (i.e., no differences for submonolayer coverages).

Surfactant Chain Length. For an insoluble polymer on the surface of a surfactant solution, there is direct contact between the surfactant's hydrocarbon chains (i.e., "tails") and the polymer. Hence, the hydrocarbon chain length of the surfactant can dramatically effect the environment the polymer experiences at the solution interface. To quantify this effect, we systematically increase the surfactant tail length by using a series of alkyltrimethylammonium bromides, C_nTAB (n = 9, 10, 12, 14, 16). All of these surfactants have the same cationic head group and, above the cmc, approximately the same surface density (45 ± 5 Å^2/molecule).[21,22] Therefore, we isolate the effect of the surfactant chain length by varying the number of carbon units from 9 to 16. In Figure 7, we plot the PDMS surface pressure isotherms for the shortest (C_9TAB), longest ($C_{16}TAB$), and middle ($C_{12}TAB$) carbon chain length of the series we tested. To further facilitate a direct comparison, we have scaled $\Delta\gamma$ by $\Delta\gamma_{max}$, which corresponds to the limiting value for large amounts of polymer (i.e., a duplex film of polymer exists on the surface). The data for all of the TAB's show the same qualitative s shape; however, as the chain length of the

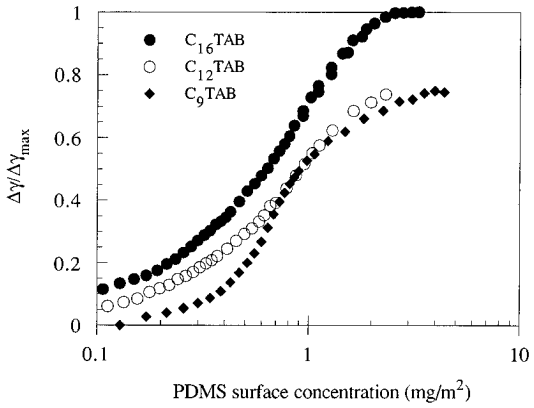

Figure 7. Scaled change in the surface tension, $\Delta\gamma/\Delta\gamma_{max}$, versus PDMS surface concentration on C_nTAB surfactant solutions (at surfactant concentrations of 3 times the cmc), with n = 9, 12, 16, at 21 °C.

tail is increased, we observe a pronounced stretching of the s form with a concomitant elevation of the $\Delta\gamma/\Delta\gamma_{max}$ plateau value. For example, on C_{16}TAB solutions, $\Delta\gamma/\Delta\gamma_{max}$ begins to rise upon the first addition of polymer, ~0.01 mg/m^2, while changes are not observed on C_9TAB solutions until a PDMS surface concentration of >0.1 mg/m^2 is reached. Moreover, on the C_9TAB solutions a pronounced plateau at $\Delta\gamma/\Delta\gamma_{max}$ ~0.75 mN/m is reached around 3 mg/m^2 of PDMS, while C_{16}TAB shows only a slight change in slope, followed by a steady continuous rise to $\Delta\gamma/\Delta\gamma_{max}$ = 1.0. The form of the curves in Figure 7 are highly reproducible. Isotherms on C_{10}TAB and C_{14}TAB solutions are not plotted in Figure 7 so that a clear comparison can be seen. In summary, the form and slope changes of the isotherm on C_{10}TAB solutions fall between those shown for C_9TAB and C_{12}TAB, while the C_{14}TAB isotherm is practically identical to that of C_{16}TAB.

Classical Spreading Coefficients. Harkins was one of the first to derive expressions which we refer to as the classical spreading coefficient.[23] This coefficient arises from the minimization of the surface free energy of the system and is represented by

$$S_{o/w} = \sigma_{aw} - \sigma_{ow} - \sigma_{oa} \quad (1)$$

where σ_{ij} corresponds to the bulk equilibrium surface or interfacial tension, and the subscripts o, w, and a signify, oil, water, and air, respectively. $S_{o/w}$ is meant to indicate that for a positive value the oil spreads over the air−water interface, while negative values imply that oil exists as a lens on the surface. The shortcoming of the classical coefficients is that they fail to account for intermediate film thicknesses that must occur between zero and a film thick enough to utilize bulk values of the tensions, σ_{ij}. Moreover, in many macroscopic systems there are additional constraints on the system (e.g., capillary pressure, finite volume, etc.) that are not accounted for in eq 1. However, recent work using Frumkin−Derjaguin wetting theory,[24,25] in conjunction with Harkins' spreading coefficients, has successfully expanded the classical ideas of a single spreading parameter based only on bulk surface tension values.[26−30] These new developments clarify some of the apparent contradictions observed when only classical ideas are used.

Although incomplete on their own, classical coefficients do provide very useful information, which taken together with other observations can lead to a better understanding of the spreading behavior. Hence, we have measured the classical spreading coefficients for each of our oil/surfactant solution combinations. Table 1 contains both the individual tension values and the calculated spreading coefficients. All surfactant−solution tensions where evaluated at three times the air−solution cmc. We have distinguished the coefficients by superscripts, I, and, eq, to indicate initial (i.e., fresh interfaces) and equilibrium (solution interfaces equilibrated with a drop of oil on the surface) conditions, respectively. As shown in Table 1, all of the initial spreading coefficients are positive. This indicates that, for fresh solutions, it is thermodynamically favorable for PDMS polymer droplets to spread on the solution−air interface. Of course there may be force barriers that prevent this from happening, in which case the system can be trapped in a metastable configuration.[27−30] Table 1 also reveals that all of the equilibrium spreading coefficients are zero within the limits of our measurement accuracy.

Table 1. Surface and Interfacial Tensions with Calculated Classical Spreading Coefficients

solution	σ_{aw}	σ_{ow}	σ_{aw}[a]	$S^{I}_{o/w}$	$S^{eq}_{o/w}$	y
water	72.8	39.1	60.6	13.1	1.0	>20
AOT	28.0	4.7	25.5	2.7	0.2	10
$C_{10}E_5$	31.5	3.5	25.1	7.4	1.1	2.0
C_9TAB	41.0	10.7	32.2	9.7	0.9	1.7
C_{10}TAB	39.8	10.4		8.8		1.5
C_{12}TAB	38.8	9.8	31.3	8.4	0.9	1.2
C_{14}TAB	37.3	9.4	30.7	7.3	0.7	0.85
C_{16}TAB	37.7	9.8	30.6	7.3	0.2	0.85

[a] Equilibrated film value.

Discussion

Since we are dealing with two components at the interface (polymer and surfactant), the change in surface tension, $\Delta\gamma$, is not strictly equivalent to the polymer surface pressure. However, for highly concentrated surfactant solutions (≫cmc), changes in the tension upon addition of polymer can be attributed solely to the polymer (i.e., we assume constant adsorption of surfactant), and we can then interpret our results in terms of the polymer surface pressure and utilize conventional two dimensional polymer theory. In this case the surface pressure, in the submonolayer region, is expected to be independent of the polymer molecular weight and to follow a scaling law of the form[4−13]

$$\pi \propto c^{y} \quad (2)$$

where π is the surface pressure ($\Delta\gamma$ in our case), c, is the polymer concentration on the surface, and the power-law exponent, y, depends on the balance of monomer−monomer and excluded volume forces. Consequently, the value of y can be used to evaluate the quality of the surface solvent, and we will refer to it as the 2-D solvency exponent. Hence, depending on the value of y, the surface is said to act as a good, Θ, or poor solvent. Good solvent behavior is expected for $y \sim 3$, and Θ solvent behavior has been predicted to occur around $y \sim 10$. Values of $y > 20$ are considered as an indication of a poor solvent,[4] while values of $y < 3$ indicate that the polymer does not strictly obey 2-D behavior and penetration into the substrate (third dimension) occurs. From this trend we see that lower values of y indicate a better mixing environment for the polymer chains.

With eq 2 in mind, we have analyzed the submonolayer region of our $\Delta\gamma$ isotherms (PDMS surface con-

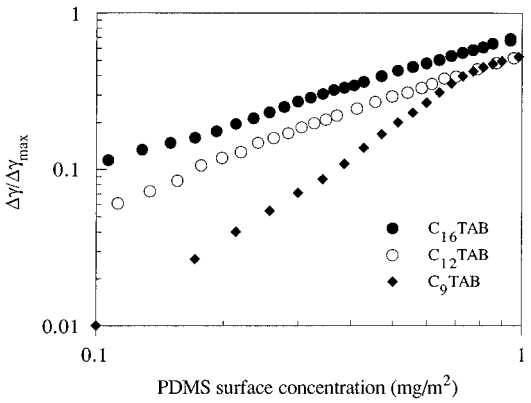

Figure 8. log−log plot of the scaled change in the surface tension, $\Delta\gamma/\Delta\gamma_{max}$, versus PDMS surface concentration on C_nTAB surfactant solutions (at surfactant concentrations of 3 times the cmc), with n = 9, 12, 16, at 21 °C.

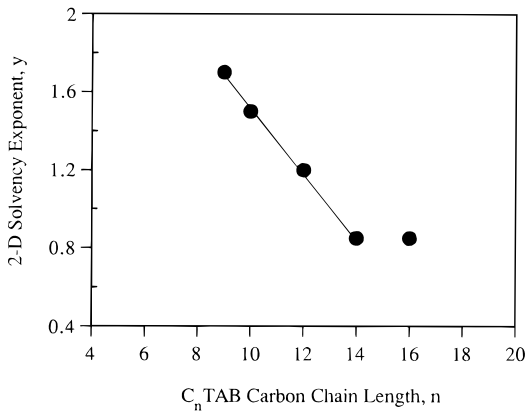

Figure 9. 2-D PDMS solvency exponent, y, on alkyltrimethylammonium bromide surfactant solutions of different surfactant chain lengths.

centrations < 1 mg/m^2) to determine the power-law exponent for each solution examined. All of the solutions produce a well-defined linear region on a log−log scale within which we are able to define a 2-D solvency exponent quite accurately. An example of the logarithmic plots used to do this can be found in Figure 8, and we tabulate the "y" values for all solutions in the last column of Table 1. For AOT and C_{12}TAB with and without salt, we find $y \sim 10$ for AOT and $y \sim 1.2$ for C_{12}TAB, regardless of whether or not salt is present in solution, and therefore we only list the no salt case in the table.

As seen in Table 1, the water surface produces the highest value of y and is therefore considered a worse 2-D solvent then any of the surfactant solution surfaces. AOT solutions are the next highest and can be classified as a Θ solvent. All of the other solutions reflect good 2-D solvent behavior of varying degrees. Moreover, these solutions have values of $y < 3$, indicating polymer penetration into the surfactant tails. As noted earlier, we observe no effect on y when electrolyte is added to solution. This suggests that electrostatic interactions between the PDMS and the surfactant head groups do not play an important role. Further confirmation of limited head-group interaction is found from the lack of any trend when comparing the different head-group types (i.e., anionic, cationic, or nonionic). However, there is a definite correlation found when the length of the carbon chain is considered. Regardless of the surfactant head group or amount of added salt, as we increase the length of the hydrocarbon tail, the exponent in eq 2 decreases. This trend is clearly demonstrated in Figure 9, where we plot the 2-D solvency exponent as a function of the carbon chain length for the alkyltrimethylammonium series (see also Figure 8). As the chain length is increased, there is a linear decrease in the 2-D solvency exponent when changing solutions from C_9TAB to C_{14}TAB; thereafter, it remains constant.

Figure 9 and Table 1 both indicate that the length of the surfactant tail plays a major role in the submonolayer spreading of PDMS on the surface of the surfactant solutions. PDMS, which is soluble in hydrocarbons, penetrates (i.e., mixes) into the surfactant tails better at surfaces that provide a more hydrocarbon-like environment. Therefore, long surfactant chain lengths promote PDMS surface mixing by allowing the polymer to interdigitate into the surfactant monolayer. This process creates a homogeneous layer of PDMS and surfactant at the surface. However, short surfactant chains at the interface force the hydrophobic PDMS closer to the water, leading to heterogeneous PDMS surface coverages as seen in BAM observations made by Mann et al.[4]

It is somewhat inconsistent to interpret spreading results for $y < 3$ and above monolayer surface concentrations (>1 mg/m^2 of PDMS), with solely a two dimensional model (i.e., eq 2). Furthermore, in our case, the thickness of the hydrocarbon layer is clearly changing with increasing surfactant chain length,[21,22] and hence the third dimension is playing an important role. Therefore, to complete our description of the PDMS spreading, we draw upon the generalized form of the spreading parameters.[26−30] Within this framework the film thickness (i.e., PDMS layer thickness) becomes a variable. The generalized form of the spreading coefficient can be derived from force balance considerations[27,29,30] or from a general free energy minimization.[28] Both methods yield the same result

$$S^{g}_{o/w} = \int_{\Pi(h_\infty)=0}^{\Pi(h)} h \, d\Pi \qquad (3)$$

which is simply a descendant of the work pioneered by Frumkin[24] and Derjaguin.[25] In eq 3 the superscript, g, on the spreading coefficient identifies it as the generalized form, Π corresponds to the disjoining pressure for the spreading phase (polymer) sandwiched between the two bulk phases (air and surfactant solution), and h is the film thickness of the spreading phase. h_∞ represents a thick film that is not influenced by disjoining forces, $\Pi(h_\infty) = 0$ (i.e., duplex polymer film). The classical expressions for the spreading coefficient are subsets of eq 3 and can be obtained by proper choice of the integration limits. In particular, the initial spreading coefficients, $S^{I}_{o/w}$ in Table 1, correspond to $h = 0$, while, $S^{eq}_{o/w}$ values are for $h = h_\infty$. Further details can be found elsewhere.[26−30]

The ideas embodied in eq 3 can be used to analyze our $\Delta\gamma$ (i.e., π) isotherms by writing the surface pressure has simply the difference between the initial and surface coated spreading coefficients, $\pi = S^{I}_{o/w} - S^{g}_{o/w}$. Invoking eq 3 with the proper integration limits yields

$$\pi = \int_{\Pi(h)}^{\Pi(h=0)} h \, d\Pi \qquad (4)$$

Hence, as pointed out by Hirasaki,[27] the film pressure and the spreading coefficient are the continuation of the same integral. Moreover, eq 4 provides us with the connection between surface pressure and disjoining pressure isotherms.

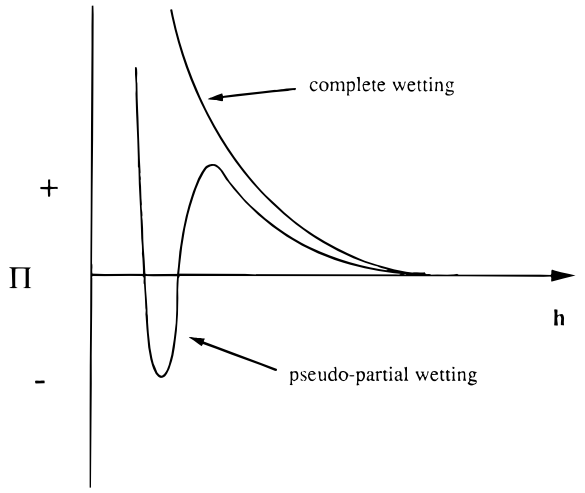

Figure 10. Schematic representation of the disjoining pressure isotherms for complete and pseudopartial wetting systems.

Considering the $\Delta\gamma/\Delta\gamma_{max}$ isotherms in Figure 7, in view of eq 4, we see that the differences can be understood in terms of the disjoining pressure isotherms. Below a carbon chain length of 14 and after a monolayer of PDMS is placed on the surface (>1 mg/m^2), $\Delta\gamma/\Delta\gamma_{max}$ displays a pronounced plateau before it reaches the final thick-film value of 1. However, once a critical surfactant chain length of 14 is reached, there is no sign of a preliminary plateau and the surface pressure rises smoothly to the duplex-film value. The $\Delta\gamma/\Delta\gamma_{max}$ plateau for the short chain solutions originates from an energy barrier which resists placing more polymer on the surface and hence thickening of the PDMS layer. Once we lengthen the surfactant tail, this barrier is dissipated and the polymer easily builds a thick duplex film. The disjoining pressure isotherms which generate this difference can be inferred from eq 4, and a schematic is sketched in Figure 10. A smoothly rising curve corresponds to a continuous interaction potential in which all film thicknesses are stable (complete wetting). This occurs for our PDMS films on C_nTAB solutions of carbon chain length greater than fourteen (n > 14). In contrast, disjoining pressure isotherms displaying a dip, with positively sloping regions which indicate unstable film thicknesses, create a resistance (i.e., a barrier) to continuous film growth. This barrier produces the plateaus seen in Figure 7. Furthermore, when the barrier is large, we can have spreading systems ($S^I_{o/w} > 0$) which still produce an oil lens. In that case the lens is in metastable equilibrium with a thin-liquid film, with the possibility of forming a finite contact angle. The conditions for this situation where realized long ago within the framework of Frumkin−Derjaguin wetting theory[31−33] and have recently been termed "pseudopartial wetting".[28] We have observed this phenomena directly for both our AOT and C_9TAB solutions. For AOT solutions we verified $S^I_{o/w} > 0$ and the presence of a PDMS precursor film, via Teflon tracer particles.[34] Afterward, we followed a PDMS lens on the surface for over 7 days. To the contrary, complete spreading of PDMS drops on C_{16}TAB solutions occurs in minutes.

Summary

$\Delta\gamma$ versus PDMS surface concentration isotherms have been performed on a wide range of surfactant solutions well above the cmc. We have investigated how different surfactant head groups and tail lengths effect the submonolayer spreading behavior of PDMS oil. The different surfactants include anionic, cationic, and nonionic. Moreover, to directly probe the effect of electrostatic forces, electrolyte is added to the solutions containing charged surfactants. We find that, above the cmc, the type of surfactant head group and the amount of charge at the interface only play a minor role.

However, in contrast to the small differences seen by altering the head group, quite large effects can be induced by changing the length of the surfactant tail. Here we study a homologous series of alkyltrimethylammonium bromides, C_nTAB (n = 9, 10, 12, 14, 16) and find that as the chain length of the surfactant tail is increased, the surface becomes a better two dimensional solvent for the PDMS submonolayer. The "solvency" exponent, predicted from polymer scaling theory, linearly decreases with carbon chain length until C_{14}TAB; thereafter, it remains constant at 0.85.

Addition of PDMS beyond the monolayer level reveals that, on short chain surfactant solutions, the spreading pressure plateaus before the final duplex film value is reached. Hence, spreading is arrested and a pseudopartial wetting condition can arise. Furthermore, a behavioral change is observed for C_nTAB carbon chains greater than 14. At and above C_{14}TAB we see no indication of a surface pressure plateau; instead PDMS films grow continuously to their thick duplex-film state. Frumkin−Derjaguin wetting theory is used to interpret these differences in terms of polymer disjoining pressure isotherms. We find that unstable polymer film-thickness regimes produce barriers to film growth which can trap the system in a metastable state. Similar behavior is responsible for the stepped profile at the spreading border of PDMS drops on solid surfaces.[26] Taken together with the previous findings of Mann et al., we show that, for equilibrium spreading of PDMS on surfactant saturated air−solution interfaces, the surfactant chain length plays a primary role.

Acknowledgment. The authors are grateful to Rhône Poulenc for partial financial support and for the polymer samples they donated.

References and Notes

(1) *Defoaming, Theory and Industrial Applications*; Garrett, P. R., Ed.; Surfactant Science Series 45; Marcel Dekker Inc.: New York, 1993.
(2) Kulkarni, R. D.; Goddard, E. D.; Kanner, B. *Ind. Eng. Chem. Fundam.* **1977**, *16*, (4), 472.
(3) Garrett, P. R. The Mode of Action of Antifoams. In *Defoaming, Theory and Industrial Applications*; Garrett, P. R., Ed., Surfactant Science Series 45; Marcel Dekker Inc.: New York, 1993; p 1.
(4) Mann, E. K. Ph.D. Thesis, Ecole Normale Superieure, Paris, France, 1992.
(5) Mann, E. K.; Lee, L. T.; Hénon, S.; Langevin, D.; Meunier, J. *Macromolecules* **1993**, *26*, 7037.
(6) Daoud, M.; Jannink, G. *J. Phys. (Paris)* **1976**, *37*, 973.
(7) Vilanove, R.; Rondelez, F. *Phys. Rev. Lett.* **1980**, *45*, 1502.
(8) Kawaguchi, K.; Yoshida, A.; Takahashi, A. *Macromolecules* **1983**, *16*, 956.
(9) Granick, S. *Macromolecules* **1985**, *18*, 1597.
(10) Kim, M. W.; Chung, T. C. *J. Colloid Interface Sci.* **1988**, *124*, 365.
(11) Vilanove, R.; Poupinet, D.; Rondelez, F. *Macromolecules* **1988**, *21*, 2880.
(12) Gaines, G. L. *Langmuir* **1991**, *7*, 834.
(13) de Gennes, P. G. *Scaling Concepts in Polymer Physics*; Cornell University Press: Ithaca, NY, 1979.
(14) Zana, R. *J. Colloid Interface Sci.* **1980**, *78*, 330.
(15) Mukerjee, P.; Mysels, K. J. *Critical Micelle Concentrations of Aqueous Surfactant Systems*; NSRDS-NBS 36, U.S. Department of Commerce: Washington, DC, 1971.

(16) Harkins, W. D.; Brown, F. E. *J. Am. Chem. Soc.* **1919**, *41*, 499.
(17) Wilkinson, M. C. *J Colloid Interface Sci.* **1972**, *40*, 14.
(18) Wilkinson, M. C.; Aronson, M. P. *J. Chem. Soc., Faraday Trans. 1* **1973**, *69*, 474.
(19) Banks, W. H. Surface Films of Polydimethyl Siloxanes on Organic Liquid Substrates. In *Gas/Liquid and Liquid/Liquid Interfaces: Proceedings of the Second International Congress of Surface Activity*; Schulman, J. H., Ed.; Butterworth Publishers: London, 1957; p 16.
(20) Adamson, A. W. *Physical Chemistry of Surfaces*, 3rd ed.; Wiley & Sons: New York, 1976.
(21) Lu, J. R.; Simister, E. A.; Thomas, R. K.; Penfold, J. *Prog. Colloid Polym. Sci.* **1993**, *93*, 92.
(22) Lee, E. M.; Thomas, R. K.; Penfold, J.; Ward, R. C. *J. Phys. Chem.* **1989**, *93*, 381.
(23) Harkins, W. D. *J. Chem. Phys.* **1941**, *9*, 552.
(24) Frumkin, A. N. *Zh. Fiz. Khim.* **1938**, *12*, 337.
(25) Derjaguin, B. V. *Zh. Fiz. Khim.* **1940**, *14*, 137.
(26) Cazabat, A. M.; Fraysse, N.; Heslot, F.; Carles, P. *J. Phys. Chem.* **19990**, *94*, 7581.
(27) Hirasaki, G. J. Thermodynamics of Thin Films and Three-Phase Contact Regions. In *Interfacial Phenomena in Petroleum Recovery*; Morrow, N. R., Ed.; Marcel Dekker Inc.: New York, 1991; p 23.
(28) Brochard-Wyart, F.; di Meglio, J. M.; Quéré, D.; de Gennes, P. G. *Langmuir* **1991**, *7*, 335.
(29) Bergeron, V.; Fagan, M. E.; Radke, C. J. *Langmuir* **1993**, *9*, 1704.
(30) Bergeron, V. Forces and Structure in Surfactant-Laden Thin-Liquid Films. Ph.D. Thesis, University of California, Berkeley, 1993.
(31) Churaev, N. V.; Starov, V. M.; Derjaguin, B. V. *J. Colloid Interface Sci.* **1982**, *89*, 16.
(32) Teletzke, G. F. Thin Liquid Films: Molecular Theory and Hydrodynamic Implications. Ph.D. Thesis, University of Minnesota, Minneapolis, 1983. Teletzke, G. F.; Scriven, L. E.; Davis, H. T. *J. Colloid Interface Sci.* **1982**, *87*, 550.
(33) Churaev, N. V. *Rev. Phys. Appl.* **1988**, *23*, 975.
(34) Bergeron, V.; Langevin, D. Precursor Film Spreading Rates of PDMS Oil on Surfactant Solutions. Submitted for publication in *Phys. Rev. Lett.*

MA950325D